Carbohydrate Polymers 99 (2014) 517–526

Contents lists available at ScienceDirect

Carbohydrate Polymers

journal homepage: www.elsevier.com/locate/carbpol

Thallium(I) sorption using Prussian blue immobilized in alginate capsules

Thierry Vincent[a], Jean-Marie Taulemesse[a], Agnès Dauvergne[a], Thomas Chanut[a], Flaviano Testa[a,b], Eric Guibal[a,*]

[a] Ecole des Mines d'Alès, Centre des Matériaux des Mines d'Alès, 6, avenue de Clavières, F-30319 Alès cedex, France
[b] Università della Calabria, Dipartimento di Ingegneria Chimica e dei Materiali, Cubo 44A, Via Pietro Bucci, I-87030 Arcavacata di Rende, Italy

ARTICLE INFO

Article history:
Received 13 July 2013
Accepted 23 August 2013
Available online 1 September 2013

Keywords:
Thallium
Alginate
Sorption isotherms
Uptake kinetics
SEM-EDX analysis

ABSTRACT

Prussian blue (PB) was immobilized in alginate capsules. The composite sorbent was used for the recovery of Tl(I) ions from slightly acidic solutions: optimum pH being close to 4. The sorption isotherm can be described by the bi-site Langmuir sorption isotherm. This means that the metal ion can be bound through two different sorption sites: one having a strong affinity for Tl(I) (probably PB), the other having a lower affinity (probably the encapsulating material). The kinetics are described by either the pseudo-second order rate equation or the Crank's equation (resistance to intraparticle diffusion). The ionic strength (increased by addition of NaCl, KCl or $CaCl_2$) slightly decreased sorption capacity. The SEM-EDX analysis of PB-alginate capsules (before and after Tl(I) sorption) shows that the PB is homogeneously distributed in the capsules and that all reactive groups remain available for metal binding.

1. Introduction

The regulations concerning the discharge of metal ions in the environment are becoming more and more stringent due to their cumulative effect in the food chain and their harmful effect on human beings. These reasons make the development of new processes for the recovery of metal ions from industrial wastewater and/or the removal from water supply facilities an important challenge. Thallium has recently received a great attention due its presence in many ores (Lopez Anton, Spears, Diaz Somoano, & Martinez Tarazona, 2013), where the leaching may cause metal release and contamination of water bodies (Xiao, Yang, Li, Zheng, & Ning, 2012); it is also produced or used in industries such as electronics, glass and drug production. The maximum contaminant level (MCL) was defined to 2 $\mu g\,L^{-1}$ by U.S. Environmental Protection Agency (considering that the maximum contaminant level goals, MCLG should be 0.5 $\mu g\,L^{-1}$). Due to its bioaccumulation in the food chain and its effects on environment and human beings (Domingo, Perello, & Gine Bordonaba, 2012; Rodriguez-Mercado & Altamirano-Lozano, 2013; Turner & Furniss, 2012); there is a major concern in recovering thallium from wastewater.

Thallium can be recovered from solution through different mechanisms including solvent extraction (Fang, Liu, Yang, Xiong, & Zang, 2009; Liu, Fang, Li, Yang, & Zang, 2005; Rajesh & Subramanian, 2006), biosorption (Memon, Memon, Solangi, & Memon, 2008; Nayak & Lahiri, 2005; Sheibani & Zare-Khormizi, 2012; Zolgharnein, Asanjarani, & Shariatmanesh, 2011), sorption on mineral sorbents(Borcia, Popa, Pavel, Dascalu, Vitelaru, & Apetrachioaei, 2011; Senol & Ulusoy, 2010; Trokhimenko, Sukhan, Nabivanets, & Ishchenko, 2000; Zhang, Huang, Liu, Zhang, & Li, 2011), or resins (Hassanien, Kenawy, El-Menshawy, & El-Asmy, 2007; Jacobson, Klitzke, McBride, Baveye, & Steenhuis, 2005). In addition, several studies have focused on the decorporation of thallium or cesium (Faustino et al., 2008), as the result of Cs or Tl radionuclide intake after nuclear accidents (such as Chernobyl (Ukraine), Goiânia (Brazil) or Fukushima (Japan)) or major radiological incident. This decorporation is generally processed by absorption of Prussian blue (PB, ferric hexacyanoferrate, $Fe_4(III)[Fe(II)(CN)_6]_3$). PB contributes to bind Cs or Tl through chemical ion exchange, physical adsorption or ion trapping. This affinity of hexacyanoferrate-based ion-exchangers (PB analogues, playing with the substitutes of Fe(III)) for Cs(I), Rb(I) or Tl(I) has been used for elaborating a number of sorbents based on free insoluble micro-particles (Ismail, El-Sourougy, Moneim, & Aly, 1998; Yang et al., 2008). Managing systems that involve micro-particles at large scale reveals difficult due to solid/liquid separation issues (in batch systems), column clogging and hydrodynamic issues (in fixed-bed systems). This is the reason that may explain that many studies focused on the immobilization of the ion-exchangers on different supports (Chang, Chau, Hu, Wang, & Liao, 2008; Nilchi, Saberi, Moradi, Azizpour, & Zarghami, 2011; Taj, Muhammad, Chaudhry,

* Corresponding author. Tel.: +33 466782734; fax: +33 466782701.
E-mail address: Eric.Guibal@mines-ales.fr (E. Guibal).

0144-8617/$ – see front matter © 2013 Elsevier Ltd. All rights reserved.
http://dx.doi.org/10.1016/j.carbpol.2013.08.076

& Mazhar, 2011; Vrtoch, Pipíška, Horník, Augustín, & Lesný, 2011). The challenge is optimizing the retention of nano- and/or microparticles while maintaining high mass transfer properties.

The present study deals with the synthesis of PB-alginate composite capsules and their testing for thallium binding from slightly acid solutions. Alginate is a biopolymer that was frequently used for immobilizing cells and enzymes (Andersen, Melvik, Gasered, Alsberg, & Christensen, 2012; Martinez et al., 2012), extractants (Guibal, Vincent, & Jouannin, 2009; Mimura, Ohta, Akiba, & Onodera, 2001), ion-exchangers (Ye et al., 2009): The material to be encapsulated is mixed with the alginate solution before being distributed into a ionotropic gelation solution (for example $CaCl_2$) (Agulhon, Markova, Robitzer, Quignard, & Mineva, 2012). This method is simpler than that proposed by Tokarev et al. (2012) who proposed the in situ synthesis of PB in the biopolymer matrix. Scanning electron microscopy (coupled with energy dispersive X-ray analysis, SEM-EDX) is used for characterizing the materials (dispersion of ion-exchanger in the capsules, distribution of thallium in the loaded capsules). Thallium sorption is investigated considering the effect of pH, and of the presence of competitor cations (i.e., K^+, Na^+ and Ca^{2+}). The sorption isotherms are discussed and modeled using the bi-site Langmuir equation. Uptake kinetics are compared for different particle sizes and different metal concentrations; kinetic profiles are modeled using the pseudo-first order and the pseudo-second order rate equations, and the Crank's equation (resistance to intraparticle diffusion).

2. Material and methods

2.1. Materials

Alginic acid (sodium salt) was supplied by Acros organics (Switzerland). Iron chloride ($FeCl_3,6H_2O$) was purchased from Chem-Lab (Belgium) and kalium hexacyanoferrate(II)-3-hydrate ($K_4[Fe(CN)_6],3H_2O$) from Riedel-de-Haen (Germany). Thallium chloride and rubidium chloride were supplied by Alpha-Aesar (France) and dissolved in sulfuric acid solution or hydrochloric acid solution (respectively). Calcium chloride ($CaCl_2,6H_2O$), sodium chloride (NaCl) were purchased from Fluka A.G. (Switzerland) and potassium chloride (KCl), from Carlo Erba (Italy).

Prussian blue was synthesized by dissolving 10 g of $K_4[Fe(CN)_6],3H_2O$ in 100 g of demineralized water and dissolving separately 26 g of $FeCl_3,6H_2O$ in 100 g of demineralized water. The potassium hexacyanoferrate solution was added drop by drop to the iron chloride solution. The final solution was then strongly agitated using an Ultra-Turrax agitator for 10 min. Finally the slurry was maintained under agitation (blade agitator) for one hour. The precipitate of PB was recovered by centrifugation (6000 rpm) and rinsed with demineralized water. The washing step was repeated four more times.

The encapsulation of the PB was operated using a two steps procedure. First a volume of 250 mL of an alginate solution (4 g of alginate in 330 g of demineralized water till complete dissolving) was added to the PB (suspended in 250 mL of water) under strong agitation (Ultra-Turrax). In a second step, the PB-alginate mixture was distributed through a thin nozzle into an ionotropic gelation solution (0.1 M calcium chloride solution). Several sizes of beads (i.e., S: 63–180 μm; M: 700–100 μm; L: 1–2 mm) were prepared using, for the small and medium size lots, a concentric injector with an air flow at the shell size: the air flow induces the fall of the composite PB-alginate drops before they fall by their own weight. The beads remained in the ionotropic gelation bath overnight before being rinsed with demineralized water and being freeze-dried. Alginate gel beads (without encapsulation of PB) were also prepared following exactly the same procedure, in order to evaluate the relative contributions of the encapsulating material and the ion-exchanger.

2.2. Characterization of materials

The morphology and the elemental distribution of mineral sorbents and Tl in the composite materials were determined with a Scanning Electron Microscope coupled with an Energy Dispersive X-ray analysis system (SEM-EDX). These data were obtained by using an Environmental Scanning Electron Microscope (ESEM) Quanta FEG 200, equipped with an OXFORD Inca 350 Energy Dispersive X-ray microanalysis (EDX) system. The SEM observations were performed on the cross-section of the capsules (made by cutting with a thin-slice cutter under a binocular microscope). Using environmental SEM allowed the direct observations of materials, without prior metallization of the samples. The topography of the samples was observed using secondary electrons while the backscattered electrons were used for the identification and localization of heavy metals at the surface of the materials (by phase contrast). SEM-EDX analysis allowed to determine the distribution of elements on the cross-section by using mapping facilities and semi-quantitative analysis of the target metal Tl and that of major component of the ion-exchanger; i.e., Fe.

In addition, the content of iron (as a tracer of the ion-exchanger) was determined by ICP-AES after mineralization. Fifty mg of sorbent were mixed under heating with 2 mL of sulfuric acid (96% w/w). One mL of hydrogen peroxide (130 volumes) was added to the slurry when appeared white smokes. The operation was repeated three other times until complete disappearance of white smokes (this corresponded to a volume of 4 mL of hydrogen peroxide). The final mixture was filtered and the dark filtrate was recovered, the volume was adjusted to 25 mL with demineralized water and the solution was analyzed by ICP-AES for determination of Fe and K content.

2.3. Sorption experiments

For the study of pH effect, 50 mL of 50 mg L^{-1} Tl(I) solutions at different pHs (between one and six) were mixed using a reciprocal shaker with 50 mg of sorbent (dried beads) for 3 days. The sorbent beads were removed by filtration on 1 μm pore size membrane and the filtrate was analyzed for residual Tl concentration using an inductively coupled plasma atomic emission spectrometer (ICP-AES, Jobin-Yvon Activa M). The pH was not controlled during the sorption but the final pH was recorded. The influence of the presence of competitor cations (Ca(II), Na(I) and K(I)) and ionic strength was tested comparing the sorption capacities and sorption yields for 80 mg Tl L^{-1} solutions at pH 4 completed with increasing amounts of salts ($CaCl_2$, NaCl and KCl)(sorbent mass: 50 mg; volume of solution: 50 mL; contact time: 3 days).

For sorption isotherms 50 mg of sorbent (m) were mixed with 50 mL (V) of Tl(I) solutions at different initial concentrations (C_0, ranging between 10 and 500 mg Tl L^{-1}) for 3 days. The pH of the solutions was set at 4. After filtration, the residual concentration (C_{eq}, mg Tl L^{-1} or mmol Tl L^{-1}) was determined by ICP-AES and the sorption capacity (q, mg Tl g^{-1} or mmol Tl g^{-1}) was calculated by the mass balance equation: $q = (C_0 - C_{eq})V/m$. For testing the sorption properties of raw alginate beads (without incorporation of PB) 100 mg of freeze-dried calcium alginate beds were maintained under agitation for 2 days in 50 mL of Tl(I) solutions at pH 4 (concentration range 100–400 mg Tl L^{-1}). Residual concentration was measured by ICP-AES and the mass balance equation was used for calculating the sorption capacity. Some experiments were also performed using equimolar concentrations of Tl(I) and Rb(I) for testing sorption selectivity.

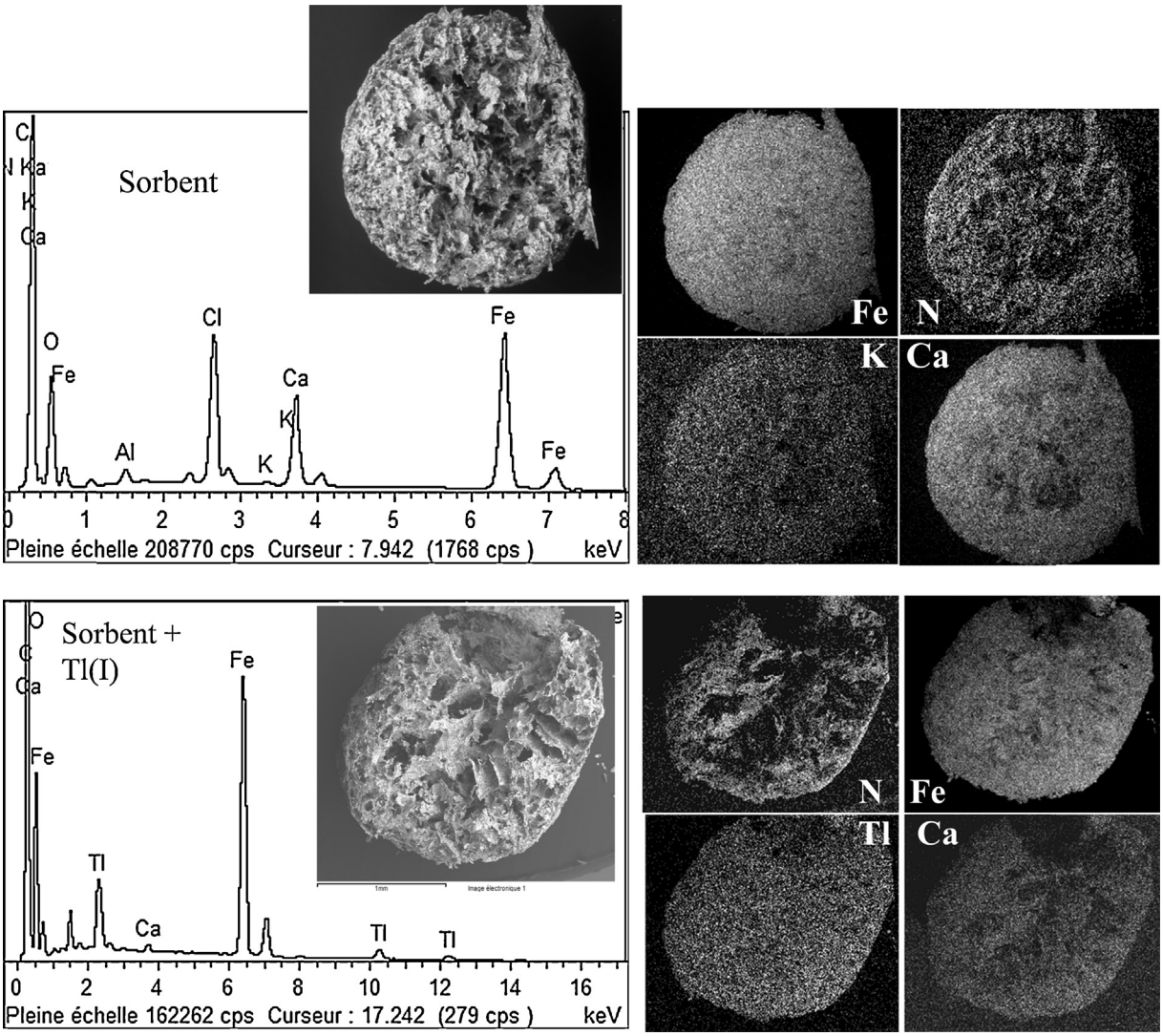

Fig. 1. SEM-EDX analysis of sorbent before and after Tl(I) sorption: XRD pattern, SEM photograph and element cartography.

For uptake kinetics a given amount of sorbent (100 or 200 mg) were mixed with 500 mL of Tl(I) solutions (C_0: 20 mg Tl L^{-1}) at pH 4. Samples were collected at fixed times and the residual concentrations were determined by ICP-AES after filtration. Experiments were performed with the different capsule sizes (dry materials).

3. Results and discussion

3.1. Sorbent characterization

The mineralization of alginate-encapsulated PB allowed analyzing the elements present in the materials, and more specifically K and Fe as the tracers of the precursor (K, for potassium ferrocyanide) and PB (Fe). Very small concentrations of K were detected in the solutions, corresponding to concentrations below 0.02 mmol K g^{-1} (less than 0.8 mg K g^{-1}). These values confirm that the precursor was negligible in the final material and that the PB was under its insoluble form. On the other hand, Fe concentration in the solid was 2.15 ± 0.04 mmol Fe g^{-1} (i.e., 119.9 ± 2.1 mg Fe g^{-1}). Based on the molecular weight of insoluble PB $(Fe(III)_4[Fe(II)(CN)_6]_3$; i.e., MW: 859.3 g mol^{-1}), this corresponds to 0.307 ± 0.005 mmol PB g^{-1} (or 263.5 ± 4.6 mg PB g^{-1}). These values are higher than those cited for the incorporation of PB analogue in silica- or glass-based nano-composites (about 10% w/w) (Delchet et al., 2012). Figs. 1 and 2 show that both Fe element (tracer of PB) and Tl element are homogeneously distributed in the whole mass of the sorbent. This means that the PB is homogeneously distributed in the composite material and that all reactive groups remain accessible for Tl(I).

3.2. pH effect

Fig. 3 shows the limited effect of pH on Tl(I) sorption capacity of alginate-encapsulated PB (from 71% to 94%, under selected experimental conditions). A small increase in recovery efficiency is observed when the pH increases: from 35 to 45 mg Tl g^{-1}. It is noteworthy that the sorption process causes a significant change in the pH above pH 3.5: in the pH range 1–3.5 the pH variation remains negligible while between pH 4 and pH 6.5 the pH tends to stabilize in the range 3.7–4 (Fig. 4). The sorbent has a kind of buffering effect above pH 4, probably due to the pK_as values of carboxylic acids (i.e., mannuronic and guluronic acids, 3.38 and 3.65, respectively (Davis, Volesky, & Mucci, 2003) present on the biopolymer. Haug observed that when a metal salt solution is added to a half neutralized sample of alginic acid the pH decrease depends on the affinity between the alginate and the metal ion (Haug, 1961). The pH variation may be due to proton binding and to metal exchange. The choice of an acidic pH is controlled not only by the efficiency

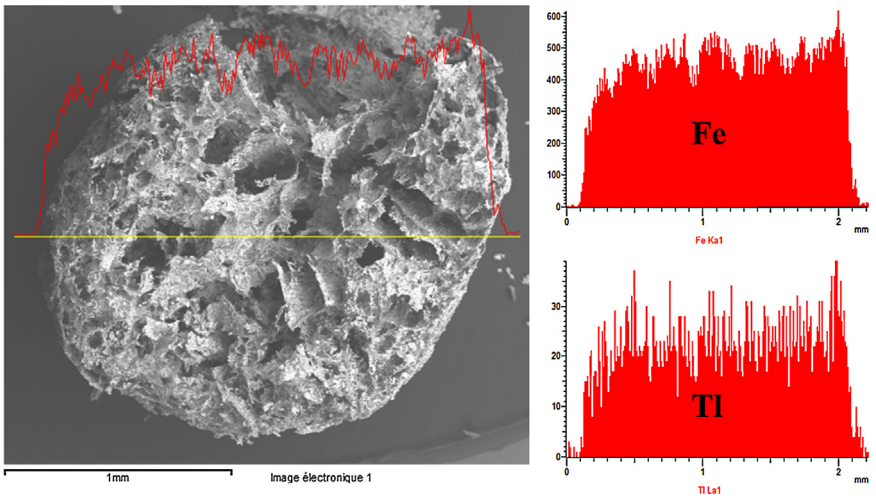

Fig. 2. SEM-EDX analysis of sorbent after Tl(I) sorption: Distribution of Fe element (tracer of the ion-exchanger) and Tl element.

of the ion-exchanger but also by the stability of the encapsulating material: in alkaline solutions the biopolymer tends to dissolve and to limit the stability of the composite sorbent.

The investigations on Tl(I) sorption using different sorbents have shown a great variability in the optimum pH: pH 1.5 for specific titanosilicate (Borcia et al., 2011), pH 2–7 for Ca-alginate beads (but pH was not controlled/measured at equilibrium) (Nayak & Lahiri, 2005), pH 3–7 for polyurethane foams loaded with molybdophosphate (Trokhimenko et al., 2000), pH 3–7 for copper ferrocyanide immobilized on mesoporous silica (Sangvanich et al., 2010), and pH 5–9 for sawdust (Memon et al., 2008).

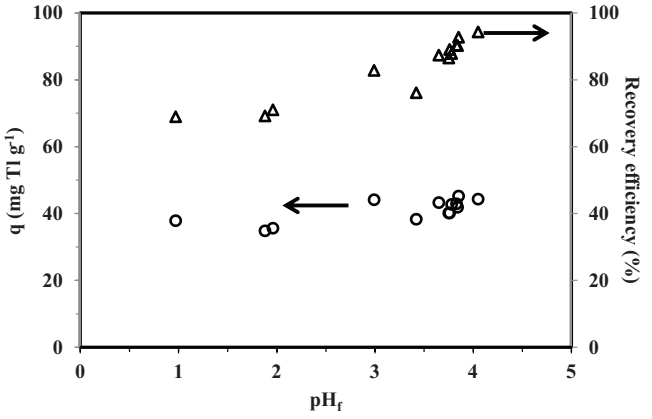

Fig. 3. pH effect on Tl(I) sorption using alginate-encapsulated PB: Sorption capacity and recovery efficiency against equilibrium pH (C_0: 50 mg Tl L^{-1}; sorbent dosage, SD: 1 g L^{-1}).

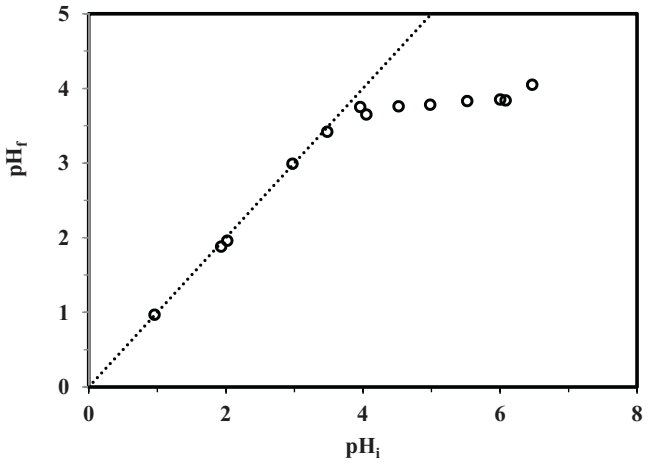

Fig. 4. pH variation during Tl(I) sorption using alginate-encapsulated PB (C_0: 50 mg Tl L^{-1}; sorbent dosage, SD: 1 g L^{-1}).

Further experiments have been performed at pH 4 based on the relative stability of the pH and the optimum efficiency of sorption.

3.3. Effect of competitor ions

The presence of competitor ions or salts in large excess compared to thallium may strongly interfere with its sorption. In order to evaluate the selectivity or the sensibility of the composite sorbent for thallium the sorption capacity of the metal was evaluated in the presence of increasing concentrations (in the range 0.1–1 M) of calcium chloride, potassium chloride and sodium chloride (Fig. 5). In the range 0–0.25 M Tl(I) sorption capacity hardly decreased while above 0.25 M, it tended to decrease (especially with calcium chloride and potassium chloride). However, the decrease in sorption capacity did not exceed 30% (from 52 to 37 mg Tl g^{-1}) when the concentration of added salts reached 1 M. Increasing the concentration of salt induced a progressive decrease of the recovery efficiency; however, this decrease did not exceed 32% (from 65% to 45%). There was not clear trend on the relative competitor effect of the different salts added to thallium solution: sodium chloride having a slightly less competitor effect than potassium and calcium chloride salts.

The distribution coefficient, K_d (mL g^{-1}) defined by the ratio q/C_{eq}, can be compared for the different systems under comparable experimental conditions. As expected increasing the concentration of competitor cations (to 0.5–1 M) resulted in a decrease of the distribution coefficient from 1.89×10^3 mL g^{-1} to $1–1.2 \times 10^3$, $0.7–0.9 \times 10^3$ and $0.9–1.2 \times 10^3$ mL g^{-1} for $CaCl_2$, KCl and NaCl, respectively. This confirms that the ionic strength of the solution and the presence of competitor cations influence Tl(I) sorption; however, even with large excess of competitor cations (about 2500 times) the sorbent maintains a good selectivity for thallium.

The fact that the composite sorbent maintained good sorption properties, even in the presence of several tens of grams of salt means that the material is quite efficient for the decontamination of complex media, such as brines, sea water and so on.

3.4. Uptake kinetics

Uptake kinetics is an important criterion for the design of a sorption system. It may be controlled by the resistance to external film

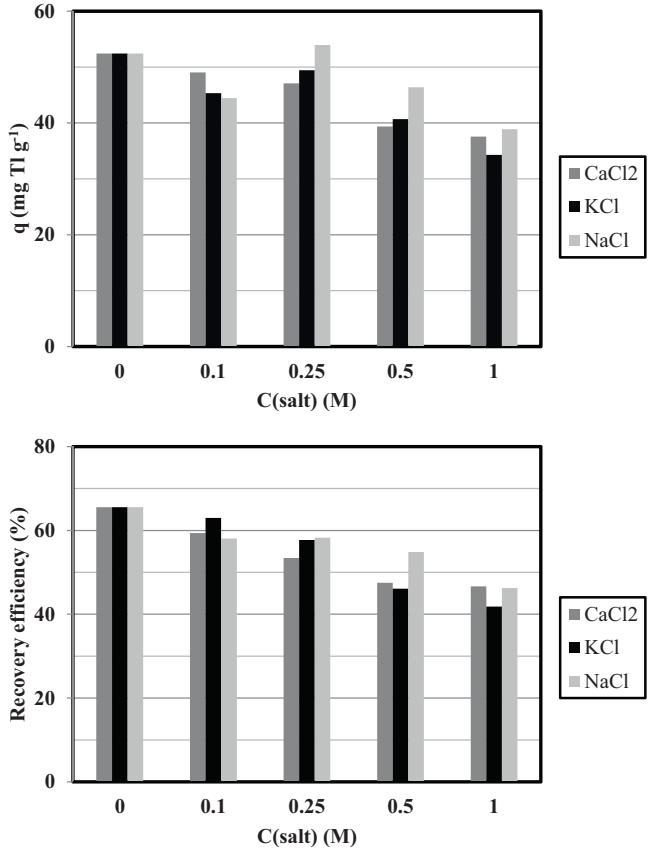

Fig. 5. Effect of increasing concentrations of salts ($CaCl_2$, KCl and NaCl) on Tl(I) sorption capacity (top) and recovery efficiency (bottom) using alginate-encapsulated PB (C_0: 80 mg Tl L^{-1}; pH: 4; sorbent dosage, SD: 1 g L^{-1}).

diffusion, the resistance to intraparticle diffusion and reaction rate. The sorption kinetics were modeled using the pseudo-first order rate equation (Sheha, 2012), the pseudo-second order rate equation (Ho, 2006), and the simplified intraparticle diffusion equation (sorption capacity plotted versus the square root of contact time) (Crank, 1975). The testing of these models showed that the pseudo-second order rate equation was systematically more appropriate for modeling the kinetic profiles.

Pseudo-first order rate equation (*PFORE*):

$$\frac{dq(t)}{dt} = k_1(q_{eq} - q(t)) \tag{1a}$$

After integration:

$$q(t) = q_{eq}(1 - e^{-k_1 t}) \tag{1b}$$

Pseudo-second order rate equation (*PSORE*)

$$\frac{dq(t)}{dt} = k_2(q_{eq} - q(t))^2 \tag{2a}$$

After integration:

$$q(t) = \frac{q_{eq}^2 k_2 t}{1 + q_{eq} k_2 t} \tag{2b}$$

where q_{eq} (mg g^{-1}) is the sorption capacity at equilibrium (calculated value from experimental data), k_2 (g mg^{-1} min^{-1}) is the pseudo-second order rate constant.

For both PFORE and PSORE the parameters were determined using the software package Mathematica® on non-linearized forms of relevant equations.

Resistance to intraparticle diffusion equation (*RIDE*)

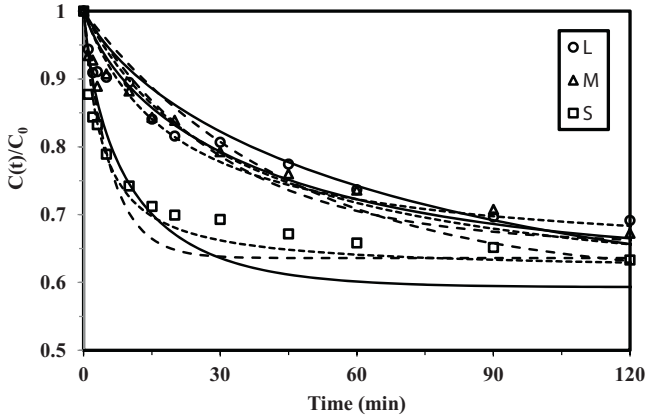

Fig. 6. Comparison of PSORE (dotted lines), PFORE (dashed lines) and RIDE (solid lines) models for the simulation of uptake kinetics using alginate-encapsulated PB (initial section of the kinetic profiles).

The intraparticle diffusion coefficient (D_e, effective diffusivity, m^2 min^{-1}) was determined using Crank's equation, assuming the solid to be initially free of metal, and the kinetics to be controlled by intraparticle diffusion resistance (Crank, 1975):

$$\frac{q(t)}{q_{eq}} = 1 - \sum_{n=1}^{\infty} \frac{6\alpha(\alpha+1)\exp\left(-D_e q_n^2 t/r^2\right)}{9 + 9\alpha + q_n^2\alpha^2} \tag{3a}$$

$q(t)$ and q_{eq} are the concentrations of the metal in the resin at time t and equilibrium, respectively, r is the radius of the particle and q_n non-zero roots of the equation:

$$\tan q_n = \frac{3q_n}{3 + \alpha q_n^2} \tag{3b}$$

This equation was applied for determining the diffusion coefficient for all kinetic data using the software package Mathematica®.

Fig. 6 shows an example of modeling of the initial sections of uptake kinetics using the three equations. Clearly, the best fit of experimental data was obtained using the pseudo-second order rate equation (PSORE). Indeed, though all models gave appropriate description of the uptake profiles in the first minutes of contact both the pseudo-first order rate equation (PFORE, or so-called Lagergren's equation) and the resistance to intraparticle diffusion equation (RIDE) tended to overestimate thallium binding in the curved part of the uptake profile. The PSORE shows much closer fit of experimental data in this critical zone of the uptake profile, especially for initial section of the curve; more discrepancies appear at long contact time (approaching the equilibrium). The difficulty to fit experimental data with the different models suggests that several mechanisms may be involved in the control of uptake kinetics, based on resistance to diffusion, on chemical reaction rate and the possible contribution of different reactive groups (see below the discussion of sorption isotherms) that may have different kinetic characteristics.

The kinetic profiles have been compared at different metal concentrations for three sizes of sorbent (Figs. 7–9). The kinetics were mainly affected by the particle size in the initial section of the curves: the kinetic profiles overlapped for medium (M) and large (L) size particles while small size particles showed much faster initial sorption. Decreasing the size of sorbent particles increases the surface of contact between the particles and the solution: this controls the resistance to film diffusion. On the other hand the size of sorbent particles may affect the resistance to intraparticle diffusion by increasing the diffusion length to the center of the particles. However, this mechanism of resistance to intraparticle diffusion is usually expected to be predominant in the second part of the kinetic

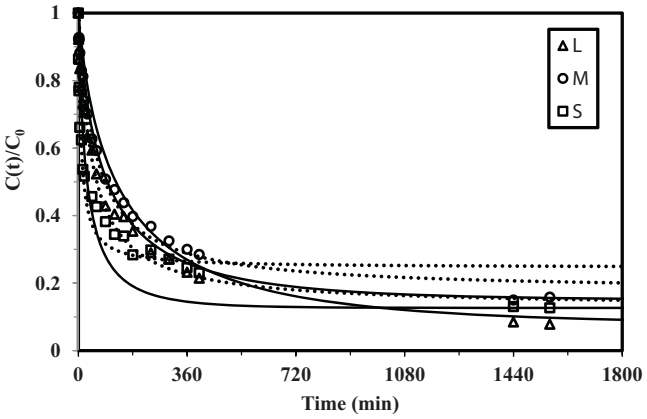

Fig. 7. Tl(I) uptake kinetics using alginate-encapsulated PB (C_0: 20 mg Tl L^{-1}; pH: 4; sorbent dosage, SD: 0.4 g L^{-1}; solid lines: modeling of the kinetic profiles using the Crank's equation (RIDE); dotted line: modeling of the kinetic profiles sing the pseudo-second order rate equation (PSORE)).

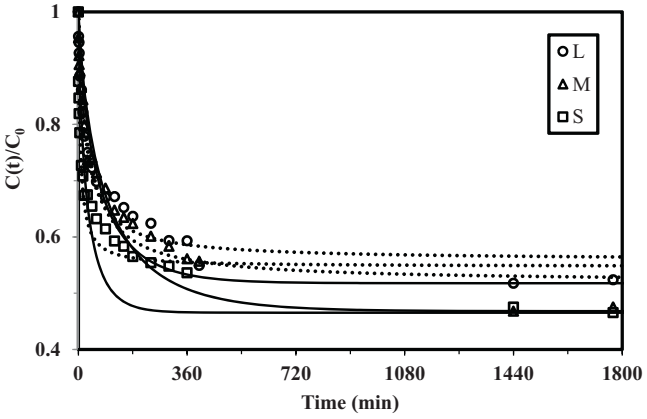

Fig. 8. Tl(I) uptake kinetics using alginate-encapsulated PB (C_0: 35 mg Tl L^{-1}; pH: 4; sorbent dosage, SD: 0.4 g L^{-1}; solid lines: modeling of the kinetic profiles using the Crank's equation (RIDE); dotted line: modeling of the kinetic profiles sing the pseudo-second order rate equation (PSORE)).

profile; the effect of particle size is thus probably attributable to a contribution of the resistance to film diffusion.

Tables 1–3 report the parameters of the different models for the different sizes of sorbent particles and for different metal concentrations. The comparison of the experimental equilibrium sorption capacity with the corresponding calculated value is a first tool for comparing PFORE and PSORE. Systematically, the PFORE model underestimated the sorption capacity at equilibrium to a greater extent than the PSORE. This is consistent with the comparison on the experimental curves with the fitted curves on Fig. 6 (also found for other experimental conditions). The PSORE kinetic coefficient (i.e., k_2) varied between 3.5×10^{-4} and 5.8×10^{-3} g mg^{-1} min^{-1}: the smallest particles having the highest

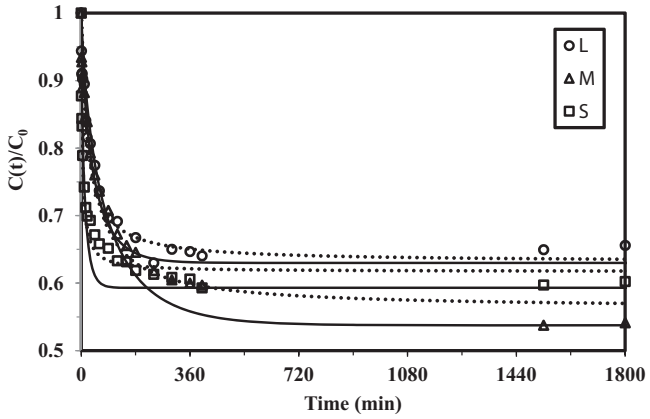

Fig. 9. Tl(I) uptake kinetics using alginate-encapsulated PB (C_0: 50 mg Tl L^{-1}; pH: 4; sorbent dosage, SD: 0.4 g L^{-1}; solid lines: modeling of the kinetic profiles using the Crank's equation (RIDE); dotted line: modeling of the kinetic profiles sing the pseudo-second order rate equation (PSORE)).

coefficients as expected from Figs. 7–9. The PFORE kinetic coefficient (i.e., k_1) varied between 0.013 and 0.17 min^{-1}; this is of the same order as the value cited for Tl(I) sorption on sawdust (i.e., 0.14 min^{-1}) (Memon et al., 2008). The PFORE was also used for fitting Tl(I) sorption kinetics using ETS-10 titanosilicate (Borcia et al., 2011). The comparison of kinetic coefficients for both PFORE and PSORE (i.e., k_1 and k_2) confirms the observation of the kinetic profiles: smallest particles have a significantly higher value than large and medium size sorbents. On the opposite hand the intraparticle diffusion coefficient decreased with decreasing the size of sorbent particles (Table 3). The variation of the intraparticle diffusion coefficient ranges between 0.27×10^{-11} and 2.21×10^{-9} m^2 min^{-1}; this is 2 to 4 orders of magnitude lower than the intraparticle diffusivity of Tl(I) in water (i.e., 1.19×10^{-7} m^2 min^{-1}) (Marcus, 1997).

3.5. Sorption isotherms

The sorption isotherms can be modeled using a huge number of equations (Tien, 1994). However, the Langmuir and the Freundlich equations are the most frequently used when considering metal sorption processes. Fig. 10 shows the sorption isotherm obtained for Tl(I) sorption on alginate encapsulated PB at pH 4. The isotherm was characterized by a steep initial slope followed by a progressive saturation.

Langmuir equation:

$$q = \frac{q_m b C_{eq}}{1 + b C_{eq}} \quad (4)$$

where q_m (sorption capacity at monolayer coverage, mg g^{-1}, or mmol g^{-1}) and b (affinity coefficient, L mg^{-1} or L $mmol^{-1}$) are the parameters of the model.

Fig. 10 shows the modeling of sorption isotherms for Tl(I) binding using the PB-alginate capsules. The dotted lines show the

Table 1
Kinetic parameters—PFORE.

C_0 (mg Tl L^{-1})	Size	$q_{e,exp}$ (mg Tl g^{-1})	$q_{e,calc}$ (mg Tl g^{-1})	$k_1 \times 10^2$ (min^{-1})	Estimated variance
20	L	47.3	39.7	1.70	18.1
20	M	44.5	38.1	1.37	12.1
20	S	46.4	37.5	8.14	24.6
35	L	42.9	35.6	3.29	15.4
35	M	47.5	38.6	2.37	22.6
35	S	46.9	38.1	11.1	28.9
50	L	44.3	41.3	3.23	14.8
50	M	54.7	47.2	2.22	27.3
50	S	49.5	44.3	17.0	20.2

Table 2
Kinetic parameters—PSORE.

C_0 (mg Tl L^{-1})	Size	$q_{e,exp}$ (mg Tl g^{-1})	$q_{e,calc}$ (mg Tl g^{-1})	$k_2 \times 10^4$ (g mg^{-1} min^{-1})	Estimated variance
20	L	47.3	44.5	3.5	6.9
20	M	44.5	43.2	4.8	3.7
20	S	46.4	40.1	27.0	11.8
35	L	42.9	39.4	10.6	5.7
35	M	47.5	43.1	7.0	9.6
35	S	46.9	40.7	38.1	13.6
50	L	44.3	44.2	11.5	9.5
50	M	54.7	52.2	58.2	12.3
50	S	49.5	46.6	53.7	6.2

Table 3
Kinetic parameters–RIDE.

C_0 (mg Tl L^{-1})	Size	$D_e \times 10^{10}$ (m^2 min^{-1})	Estimated variance
20	L	1.52	0.084
20	M	0.78	0.045
20	S	0.043	0.265
35	L	10.8	0.158
35	M	2.3	0.155
35	S	0.15	0.369
50	L	22.1	0.091
50	M	3.1	0.124
50	S	0.53	0.168

Table 4
Tl(I) sorption isotherms—parameters of the Langmuir and bi-site Langmuir models.

Langmuir			Langmuir bi-site				
q_m (mg Tl g^{-1})	b (L mg^{-1})	MSR	q_{m1} (mg Tl g^{-1})	b_1 (L mg^{-1})	q_{m2} (mg Tl g^{-1})	b_2 (L mg^{-1})	MSR
103.0	0.0776	186.2	50.9	1.65	74.1	0.0075	15.5
31.5	0.0172	18.9	20.0	0.917	21.5	0.0061	8.97

MSR: Mean square of residuals $\left(\sum_1^n (q_{c,i} - q_{exp,i})^2/n\right)$.

modeling of experimental data with the Langmuir equation: the plot overestimates the sorption capacity at intermediary section of the curve. A better fit of experimental data can be obtained using the Langmuir bi-site equation (Butewicz, Gavilan, Pestov, Yatluk, Trochimczuk, & Guibal, 2010; Escudero, Robitzer, Di Renzo, & Quignard, 2009). This behavior is typical of systems involving several types of sorption sites with different adsorption energy. The concept of bi-site Langmuir equation was first developed to take into account the heterogeneities of sorbents (presence of different groups with different affinity for target solute). Differences in energy adsorption may also result from changes in the metal species that are adsorbed on the sorbent. This makes the concept of bi-site Langmuir equation extendable to systems involving also the binding of different types of solute (including a solute present under different forms with different affinities for sorption sites).

Assuming that several sites could be involved in the binding (or that several species could be bound with different affinity), the Langmuir equation becomes:

Langmuir bi-site equation

$$q = \frac{q_{m,1} b_1 C_{eq}}{1 + b_1 C_{eq}} + \frac{q_{m,2} b_2 C_{eq}}{1 + b_2 C_{eq}} \quad (5)$$

where ($q_{m,1}$, b_1) and ($q_{m,2}$,b_2) are the parameters for the two types of sorption sites.

The affinity coefficients (b_1 and b_2) may be significantly different reflecting the differences in strength of the interaction of the solute with these different sorption sites (or different metal species). The parameters of the Langmuir bi-site model are presented in Table 4. The fitted curve (using the bi-site model) is represented by bold lines in Fig. 10.

Freundlich equation

$$q = k_F \times C_{eq}^{1/n} \quad (6)$$

where k_F ($mg^{1-1/n}$ $L^{1/n}$ g^{-1}) and n are the parameters of the Freundlich model.

Fig. 10 shows that the Freundlich equation is superimposed to the Langmuir bi-site fit on a wide range of concentration but tends to diverge above a residual concentration of 250 mg Tl g^{-1} (Table 5). The Freundlich equation is a power-function that shows an exponential trend while the Langmuir bi-site equation has an asymptotic trend more consistent with experimental data.

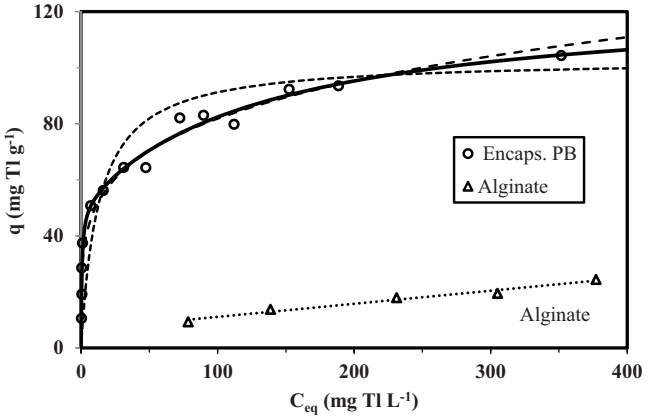

Fig. 10. Tl(I) sorption isotherm at pH 4 using alginate-encapsulated PB—modeling of experimental data with Langmuir equation (dashed line), Langmuir bi-site equation (solid line) and Freundlich equation (dashed line) (models' parameters are summarized in Tables 4 and 5)/Tl(I) sorption at pH 4 using alginate beads (dotted line: linear isotherm).

Table 5
Tl(I) and Rb(I) sorption isotherms—parameters of the Freundlich model.

k ($mg^{1-1/n}\,L^{1/n}\,g^{-1}$)	n (dimensionless)	MSR
29.9	4.57	27.5
12.0	5.51	8.29

MSR: Mean square of residuals $\left(\sum_1^n (q_{c,i} - q_{exp,i})^2/n\right)$.

The comparison of MSR (mean square of residuals) confirms that the three models can be ranked according to: Langmuir bi-site equation > Freundlich equation ≫ Langmuir equation. The Langmuir bi-site suggests (a) the contribution of two different types of sorption sites that could be the ion-exchanger and the matrix (i.e., alginate) with different affinities for the target metal, and/or (b) the sorption of different species of the metal (due to complexation, hydrolysis etc.). In the present case, at pH 4, under selected experimental conditions, thallium is free in solution: hydrolysis complexes and chloride complexes are not stable (Baes & Mesmer, 1976). The heterogeneities (which could explain the good fit of experimental data by the Langmuir bi-site equation) can thus be attributed to the presence of two types of sorption sites: the ion-exchanger (i.e., PB) and the alginate matrix. Alginate gel beads have been tested for radionuclides (including thallium) (Nayak & Lahiri, 2005): the sorption affinity is relatively limited but non negligible. This is consistent with the parameters found for the two kinds of sites in the modeling of experimental data with the Langmuir bi-site equation: both sites would have comparable sorption capacities (51 and 74 mg Tl g^{-1}) but strongly different values for the affinity coefficients (1.65 vs. 0.0075 L mg^{-1}). Alginate material is supposed to be poorly reactive for Tl(I) compared to PB (Nayak & Lahiri, 2005; Yang et al., 2008). In order to verify this hypothesis complementary sorption experiments have been performed at pH 4 using calcium alginate gel beads. Under selected experimental conditions (initial metal concentration range: 100–400 mg Tl L^{-1}; sorbent dosage: 2 g L^{-1}) the sorption yield remained almost constant (i.e., 15 ± 3%), the sorption capacity increased almost linearly (but remaining below 28 mg Tl g^{-1}) and the distribution coefficient varied between 64 and 110 (i.e., far below the values reached with alginate-encapsulated PB).

The good fit of experimental data by the Freundlich equation confirms that the sorbent material can be considered as heterogeneous: among the different hypotheses associated with the Freundlich model is the possibility to sorb the target sorbate through different sites with different sorption energies. Though the mathematical fit of experimental data does not necessarily mean that the hypotheses of the model are respected this is consistent with the structure of the material and with the co-existence of different materials that could interact with thallium ions. Complementary experiments have been performed using alginate beads (free of PB) and Fig. 11 shows that the sorption was almost linear and sorption capacity did not exceed 25 mg Tl g^{-1}. These results are consistent and demonstrate the co-existence of two types of reactive groups that are active for thallium binding: PB for the "strong" sorption of Tl(I) and alginate encapsulating material that contributes to a marginal sorption (especially at high metal residual concentration).

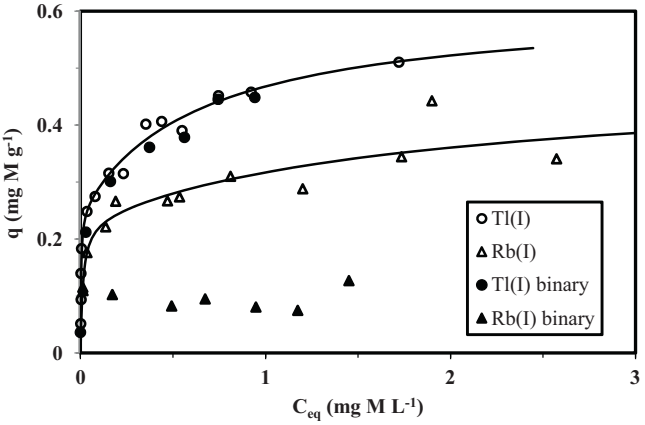

Fig. 11. Comparison of Tl(I) and Rb(I) sorption isotherms in mono-component solutions (open symbols) and bi-component solutions (closed symbols) at pH 4.

The maximum sorption capacity is close to 104 mg Tl g^{-1}. This value is consistent with those obtained with pistachio hull (Sheibani & Zare-Khormizi, 2012) (for Tl(III)), lower than those obtained with modified sugar beet pulp (about 185 mg Tl g^{-1}) (Zolgharnein et al., 2011), and higher than those obtained with mineral sorbent or ion-exchangers (Borcia et al., 2011; Sangvanich et al., 2010), or sawdust (Table 6) (Memon et al., 2008). Based on the content of PB in the composite material (i.e., 26.4% in weight) the sorption capacity is about 395 mg Tl g^{-1} PB (close to 1.93 mmol Tl g^{-1} PB). This is far from the value cited by Yang et al. (2008) for the binding of thallium to PB (i.e., 1400 mg Tl g^{-1} at pH 7.5, in vitro experiments). The molar ratio between thallium and PB at saturation of the composite sorbent is thus close to 1.65 mol Tl mol^{-1} PB (assuming that the insoluble PB is formed of $Fe(III)_4[Fe(II)(CN)_6]_3$; i.e., MW: 859.3 g mol^{-1}). Thallium binding may occur through different mechanisms including ion exchange (involving hydrogen from water bound into PB crystal lattice or alkali metal impurities bound to PB during the synthesis procedure), adsorption on the crystal lattice or ion trapping in the cavities of the ion-exchanger (Yang et al., 2008). It is thus difficult to establish a theoretical molar ratio between PB and thallium and to correlate the maximum sorption capacity to the PB content in the composite material. The distribution coefficient (K_d, mL g^{-1}) corresponds to the slope of the isotherm at low concentration; this can be calculated by q/C_{eq} (at low residual metal concentration) and approximated by $q_m \times b$ (from the Langmuir equation). The distribution coefficient is close to 8000 mL g^{-1}.

In order to verify the selectivity of the sorbent for Tl(I) against other cations that have affinity for PB some experiments were carried out in binary solutions containing equimolar concentrations of Tl(I) and Rb(I). Fig. 11 compares the isotherms obtained in

Table 6
Comparison of sorption performance for different materials.

Sorbent	pH range	q_m (mg Tl g^{-1})	b (L mg^{-1})	Thallium	Reference
Pistachio hull	5	125	0.768	III	Sheibani and Zare-Khormizi (2012)
Multiwall carbon nanotubes	7	3–31.5	0.005–0.2	III	Rehman, Ullah, Kamali, Ali, Yerlikaya, & Rehman, 2012)
Modified sugar beet pulp	5–9	185.2	0.002	I	Zolgharnein et al. (2011)
Titanium silicate (ETS-10)	1.5			I	Borcia et al. (2011)
Cu(II) ferrocyanide-mesoporous silica	7.8	28.3		I	Sangvanich et al. (2010)
Prussian blue	7.8	5.8		I	Sangvanich et al. (2010)
Prussian blue NP	7.5	1400			Yang et al. (2008)
Modified sawdust	6–9	2.7–13.2	5.4–9.1	I	Memon et al. (2008)
Alginate-PB	4	103	0.078	I	This work

mono- and bi-component solutions (see Tables 4–5 for prameters). It is noteworthy that the sorption of Rb(I) by alginate beads (free of PB) was quite low (below 7 mg Rb g^{-1}, even with a Rb(I) residual concentration higher than 400 mg Rb L^{-1}, not shown). The comparison of the sorption isotherms for mono-component solutions clearly shows that the sorbent has a marked preference for Tl(I) than for Rb(I) (as indicated by both maximum sorption capacity and affinity coefficient). This result is confirmed by the sorption isotherms obtained from binary solutions: while Tl(I) sorption isotherm was hardly affected by the presence of Rb(I); the sorption capacities for Rb(I) were drastically reduced (below 0.13 mmol Rb g^{-1} while in mono-component solutions the maximum sorption capacity was closed to 0.34 mmol Rb g^{-1}). Such a preference of the sorbent (and more specifically PB) for Tl(I) cannot be explained by the differences in the ionic radius (149 and 150 pm for Rb(I) and Tl(I), respectively) nor the Stokes radius (4.7 and 5.0 pm for Rb(I) and Tl(I), respectively), which were quite similar for the two metal ions (Marcus, 1997). In the case of Tl(I) solvent extraction using selective crown ethers Ouchi and Hakushi (1996) also observed a preference for Tl(I) versus Rb(I) though the cation diameters were so close. Much more significant differences were reported considering the coordinating properties of these metal ions: the softness parameters are quite different for Rb(I) (i.e., −0.53) and Tl(I) (i.e., +0.20).(Marcus, 1997) These comparisons make the interpretation of selectivity mechanism difficult since the main mechanisms suspected to be involved in metal binding are entrapping in the ion-exchanger cage or chemical ion exchange.

4. Conclusions

The composite material prepared by encapsulation of Prussian blue into calcium alginate capsules is efficient for recovering thallium(I) ions from slightly acidic solutions (i.e., optimum pH 4). The pH hardly changed the sorption capacity in the range 1–4. The presence of competitor cations (i.e., Ca(II), Na(I) or K(I)) slightly reduced thallium sorption capacity but even with a 2500 times excess the distribution coefficients remained quite high around 10^3. The presence of Rb(I) did not significantly influence Tl(I) sorption while Tl(I) strongly decreased Rb(I) uptake. The sorption isotherm showed a steep initial slope followed by a progressive saturation of the sorbent. The isotherm can be described by the Freundlich equation and preferentially by the Langmuir bi-site model. Two reactive groups may operate: PB with a strong affinity for thallium and calcium alginate with a much lower affinity. The pseudo-second order rate equation fitted well experimental data (better than the pseudo-first order rate equation). The size of sorbent particles has a significant impact on the kinetic profiles, especially for small size particles that showed fast decrease of thallium concentration followed by a stabilization of sorption efficiency at a slightly higher level than those obtained (much slowly) with medium and large size particles. The resistance to film diffusion is suspected to play a role on the control of uptake kinetics. On the other hand, the Crank's equation (representative of the resistance to intraparticle diffusion mechanism) gave a good fit of the first section of the kinetic profiles (within the first hours) for large and medium size particles but completely failed to describe the kinetic profile of small size particles.

References

Agulhon, P., Markova, V., Robitzer, M., Quignard, F., & Mineva, T. (2012). Structure of alginate gels: Interaction of diuronate units with divalent cations from density functional calculations. *Biomacromolecules*, *13*(6), 1899–1907.

Andersen, T., Melvik, J. E., Gasered, O., Alsberg, E., & Christensen, B. E. (2012). Ionically gelled alginate foams: Physical properties controlled by operational and macromolecular parameters. *Biomacromolecules*, *13*(11), 3703–3710.

Baes, C. F., Jr., & Mesmer, R. E. (1976). *Hydrolysis of cations*. NY: Wiley.

Borcia, C., Popa, K., Pavel, C. C., Dascalu, A., Vitelaru, C., & Apetrachioaei, B. A. (2011). Sorption of thallous ion from acidic aqueous solutions onto ETS-10 titanosilicate. *Journal of Radioanalytical and Nuclear Chemistry*, *288*(1), 25–30.

Butewicz, A., Gavilan, K. C., Pestov, A. V., Yatluk, Y., Trochimczuk, A. W., & Guibal, E. (2010). Palladium and platinum sorption on a thiocarbamoyl-derivative of chitosan. *Journal of Applied Polymer Science*, *116*(6), 3318–3330.

Chang, C.-Y., Chau, L.-K., Hu, W.-P., Wang, C.-Y., & Liao, J.-H. (2008). Nickel hexacyanoferrate multilayers on functionalized mesoporous silica supports for selective sorption and sensing of cesium. *Microporous and Mesoporous Materials*, *109*(1–3), 505–512.

Crank, J. (1975). *The mathematics of diffusion*. Oxford, GB: Oxford University Press.

Davis, T. A., Volesky, B., & Mucci, A. (2003). A review of the biochemistry of heavy metal biosorption by brown algae. *Water Research*, *37*(18), 4311–4330.

Delchet, C., Tokarev, A., Dumail, X., Toquer, G., Barre, Y., Guari, Y., Guerin, C., Larionova, J., & Grandjean, A. (2012). Extraction of radioactive cesium using innovative functionalized porous materials. *RSC Advances*, *2*(13), 5707–5716.

Domingo, J. L., Perello, G., & Gine Bordonaba, J. (2012). Dietary intake of metals by the population of Tarragona County (Catalonia, Spain): Results from a duplicate diet study. *Biological Trace Element Research*, *146*(3), 420–425.

Escudero, R. R., Robitzer, M., Di Renzo, F., & Quignard, F. (2009). Alginate aerogels as adsorbents of polar molecules from liquid hydrocarbons: Hexanol as probe molecule. *Carbohydrate Polymers*, *75*(1), 52–57.

Fang, D.-W., Liu, X.-Z., Yang, J.-Z., Xiong, Y., & Zang, S.-L. (2009). Thermodynamics of solvent extraction of thallium with diethylhexyl phosphoric acid. *Physics and Chemistry of Liquids*, *47*(3), 274–281.

Faustino, P. J., Yang, Y., Progar, J. J., Brownell, C. R., Sadrieh, N., May, J. C., Leutzinger, E., Place, D. A., Duffy, E. P., Houn, F., Loewke, S. A., Mecozzi, V. J., Ellison, C. D., Khan, M. A., Hussain, A. S., & Lyon, R. C. (2008). Quantitative determination of cesium binding to ferric hexacyanoferrate: Prussian blue. *Journal of Pharmaceutical and Biomedical Analysis*, *47*(1), 114–125.

Guibal, E., Vincent, T., & Jouannin, C. (2009). Immobilization of extractants in biopolymer capsules for the synthesis of new resins: A focus on the encapsulation of tetraalkyl phosphonium ionic liquids. *Journal of Materials Chemistry*, *19*(45), 8515–8527.

Hassanien, M. M., Kenawy, I. M., El-Menshawy, A. M., & El-Asmy, A. A. (2007). Separation and preconcentration of gallium(III), indium(III), and thallium(III) using new hydrazone-modified resin. *Analytical Sciences*, *23*(12), 1403–1408.

Haug, A. (1961). The affinity of some divalent metals to different types of alginates. *Acta Chemica Scandinavica*, *15*, 1794–1795.

Ho, Y. S. (2006). Second-order kinetic model for the sorption of cadmium onto tree fern: A comparison of linear and non-linear methods. *Water Research*, *40*(1), 119–125.

Ismail, I., El-Sourougy, M., Moneim, N., & Aly, H. (1998). Preparation, characterization, and utilization of potassium nickel hexacyanoferrate for the separation of cesium and cobalt from contaminated waste water. *Journal of Radioanalytical and Nuclear Chemistry*, *237*(1), 97–103.

Jacobson, A. R., Klitzke, S., McBride, M. B., Baveye, P., & Steenhuis, T. S. (2005). The desorption of silver and thallium from soils in the presence of a chelating resin with thiol functional groups. *Water Air and Soil Pollution*, *160*(1–4), 41–54.

Liu, X. Z., Fang, D. W., Li, J., Yang, X. Z., & Zang, S. L. (2005). Thermodynamics of solvent extraction of thallium. *Journal of Phase Equilibria and Diffusion*, *26*(4), 342–346.

Lopez Anton, M. A., Spears, D. A., Diaz Somoano, M., & Martinez Tarazona, M. R. (2013). Thallium in coal: Analysis and environmental implications. *Fuel*, *105*, 13–18.

Marcus, Y. (1997). *Ion properties*. New York, NY: Marcel Dekker, Inc.

Martinez, C. J., Kim, J. W., Ye, C., Ortiz, I., Rowat, A. C., Marquez, M., & Weitz, D. (2012). A microfluidic approach to encapsulate living cells in uniform alginate hydrogel microparticles. *Macromolecular Bioscience*, *12*(7), 946–951.

Memon, S. Q., Memon, N., Solangi, A. R., & Memon, J.-u.-R. (2008). Sawdust: A green and economical sorbent for thallium removal. *Chemical Engineering Journal*, *140*(1–3), 235–240.

Mimura, H., Ohta, H., Akiba, K., & Onodera, Y. (2001). Selective uptake and recovery of palladium by biopolymer microcapsules enclosing Cyanex 302 extractant. *Journal of Nuclear Science and Technology*, *38*(5), 342–348.

Nayak, D., & Lahiri, S. (2005). Biosorption of toxic, heavy, no-carrier-added radionuclides by calcium alginate beads. *Journal of Radioanalytical and Nuclear Chemistry*, *267*(1), 59–65.

Nilchi, A., Saberi, R., Moradi, M., Azizpour, H., & Zarghami, R. (2011). Adsorption of cesium on copper hexacyanoferrate-PAN composite ion exchanger from aqueous solution. *Chemical Engineering Journal*, *172*(1), 572–580.

Ouchi, M., & Hakushi, T. (1996). Cation binding by thallium(I) selective crown ethers. *Coordination Chemistry Reviews*, *148*(0), 171–181.

Rajesh, N., & Subramanian, M. S. (2006). A study of the extraction behavior of thallium with tribenzylamine as the extractant. *Journal of Hazardous Materials*, *135*(1–3), 74–77.

Rehman, S. U., Ullah, N., Kamali, A. R., Ali, K., Yerlikaya, C., & Rehman, H. U. (2012). Study of thallium(III) adsorption onto multiwall carbon nanotubes. *New Carbon Materials*, *27*(6), 409–415.

Rodriguez-Mercado, J. J., & Altamirano-Lozano, M. A. (2013). Genetic toxicology of thallium: A review. *Drug and chemical toxicology*, *36*(3), 369–383.

Sangvanich, T., Sukwarotwat, V., Wiacek, R. J., Grudzien, R. M., Fryxell, G. E., Addleman, R. S., Timchalk, C., & Yantasee, W. (2010). Selective capture of cesium and thallium from natural waters and simulated wastes with copper ferrocyanide functionalized mesoporous silica. *Journal of Hazardous Materials*, *182*(1–3), 225–231.

Senol, Z. M., & Ulusoy, U. (2010). Thallium adsorption onto polyacryamide-aluminosilicate composites: A Tl isotope tracer study. *Chemical Engineering Journal*, *162*(1), 97–105.

Sheha, R. R. (2012). Preparation and performance of a novel composite as a reactive resin for copper retention. *Chemical Engineering Journal*, *213*, 163–174.

Sheibani, A., & Zare-Khormizi, M. (2012). Application of factorial design for adsorption of thallium(III) ion from aqueous solutions by pistachio hull. *Indian Journal of Chemical Technology*, *19*(1), 48–51.

Taj, S., Muhammad, D., Chaudhry, M. A., & Mazhar, M. (2011). Lithium, rubidium and cesium ion removal using potassium iron(III) hexacyanoferrate(II) supported on polymethylmethacrylate. *Journal of Radioanalytical and Nuclear Chemistry*, *288*(1), 79–88.

Tien, C. (1994). *Adsorption calculations and modeling*. Newton, MA: Butterworth-Heinemann.

Tokarev, A., Agulhon, P., Long, J., Quignard, F., Robitzer, M., Ferreira, R. A. S., Carlos, L. D., Larionova, J., Guerin, C., & Guari, Y. (2012). Synthesis and study of Prussian blue type nanoparticles in an alginate matrix. *Journal of Materials Chemistry*, *22*(38), 20232–20242.

Trokhimenko, O. M., Sukhan, V. V., Nabivanets, B. I., & Ishchenko, V. B. (2000). Sorption preconcentration of thallium(I) on polyurethane foam modified with molybdophosphate. *Journal of Analytical Chemistry*, *55*(7), 626–629.

Turner, A., & Furniss, O. (2012). An evaluation of the toxicity and bioaccumulation of thallium in the coastal marine environment using the macroalga, *Ulva lactuca*. *Marine Pollution Bulletin*, *64*(12), 2720–2724.

Vrtoch, Ľ., Pipíška, M., Horník, M., Augustín, J., & Lesný, J. (2011). Sorption of cesium from water solutions on potassium nickel hexacyanoferrate-modified *Agaricus bisporus* mushroom biomass. *Journal of Radioanalytical and Nuclear Chemistry*, *287*(3), 853–862.

Xiao, T., Yang, F., Li, S., Zheng, B., & Ning, Z. (2012). Thallium pollution in China: A geo-environmental perspective. *Science of the Total Environment*, *421*, 51–58.

Yang, Y., Faustino, P. J., Progar, J. J., Brownell, C. R., Sadrieh, N., May, J. C., Leutzinger, E., Place, D. A., Duffy, E. P., Yu, L. X., Khan, M. A., & Lyon, R. C. (2008). Quantitative determination of thallium binding to ferric hexacyanoferrate: Prussian blue. *International Journal of Pharmaceutics*, *353*(1–2), 187–194.

Ye, X. S., Wu, Z. J., Li, W., Liu, H. N., Li, Q., Qing, B. J., Guo, M., & Go, F. (2009). Rubidium and cesium ion adsorption by an ammonium molybdophosphate-calcium alginate composite adsorbent. *Colloids and Surfaces a—Physicochemical and Engineering Aspects*, *342*(1–3), 76–83.

Zhang, L., Huang, T., Liu, X., Zhang, M., & Li, K. (2011). Selective solid-phase extraction of trace thallium with nano-Al_2O_3 from environmental samples. *Journal of Analytical Chemistry*, *66*(4), 368–372.

Zolgharnein, J., Asanjarani, N., & Shariatmanesh, T. (2011). Removal of thallium(I) from aqueous solution using modified sugar beet pulp. *Toxicological and Environmental Chemistry*, *93*(2), 207–214.